

MODELING OF WELDING PARAMETERS ON ULTIMATE TENSILE STRENGTH IN Nd: YAG OF TITANIUM WITH Ti-6Al-7Nb ALLOYS WITH RSM

JASSIM M. SALMAN¹, SAAD HAMEED AL-SHAFAIE² & WEAAM MOHAMMED MOSLIM³

^{1,2}Professor, Department of Metallurgical Engineering, College of Materials Engineering, University of Babylon, Iraq

³Research Scholar, Department of Metallurgical Engineering, College of Materials Engineering, University of Babylon, Iraq

Original Article

ABSTRACT

In the present work, Response Surface Methodology is used to investigate the effect of four input variables, namely: type of workpiece (WP), pulse energy (PE), pulse duration (Ton), welding speed (WS) and on the ultimate tensile strength (UTS) in YAG laser welding process. To study the proposed second-order polynomial model for UTS, a Central Composite Design is used for estimating the model coefficients of the four input factors on UTS. Experiments were conducted on Cp- Ti alloy with Ti-6Al-7Nb alloy. The significant coefficients are obtained by performing an Analysis of Variance at the 5 % level of significance. The results revealed that UTS is more influenced by type of workpiece, pulse energy, pulse duration, welding speed and few of their interactions. A mathematical regression model was developed to predict the UTS in YAG laser welding. Also, the developed model could be used for the selection of the levels in this process for saving in welding time. The model sufficiency is very satisfactory as the Coefficient of Determination (R^2) is found to be 98.35% and adjusted R^2 -statistic (R^2_{adj}) 97.34%.

KEYWORDS: Pulsed Nd- YAG Laser Welding, Ti, Ti-6Al-7Nb Alloy, UTS, MODELLING & RSM

Received: Dec 01, 2019; **Accepted:** Dec 20, 2019; **Published:** Mar 24, 2020; **Paper Id.:** IJMPERDAPR202071

1. INTRODUCTION

Pulsed Nd: YAG laser; welding has especially attracted attention; recently in many academic research and industry applications [1]. Laser Beam welding is a method of fusing two pieces of metal together by using a high-heat laser. This technique uses one of two types of welding; equipment: a solid state welder or a gas laser welder. These machines both create a precise bond by emitting a dense photon beam that; can work with both thin and thick pieces; of metal. This type of welder is popular in producing airplanes, cars and spacecraft 002C; but has a few; disadvantages that prohibit it from; working in all industries welding with laser beams works because; of a dense beam of photons; that each; type of machine produces. This light ray; heats metals up quickly so that the two pieces fuse together into one unit. The light beam is very small and focused, so the metal weld; also cools very quickly. Laser beam welding machines can give off a continuous beam to work with; thicker metals, or short pulsing bursts to; bind thinner materials[2]. Nowadays, laser beam is applied for the various processes like heat treatment, material removal, alloying, cladding, cutting, drilling and welding;. Among all these processes, laser welding is considered as widely recommended process for the joining of similar dissimilar metals . Laser beam welding is a welding process used to join two metals by the use of a laser source. The laser source provides intense and high density heat source, allowing for narrow, deep weld bead with high welding scan speed, now-a-days it has wide applications in various metal working industries due to its advantageous effects over other machining operations . Laser beam welding has high power density and a small heat affected zone due to high heating and cooling rates . Laser beam welding is a versatile process, which can weld almost all materials including aluminum, titanium, carbon steels, HSLA steels and stainless steel. The laser beam is an efficient technique to join different metals. This can join; metals at the surface level and also at depth and produce very strong welding. It can be coupled with conventional welding processes to give required weld quality. The laser welding offers; many features which make it an attractive alternative to conventional processes. Continuous or pulsed laser beam may be used depending upon the various applications in metal industries. Thin materials are welded by millisecond-long pulses while continuous laser systems are used for deep welds. The laser welding process operates at very high scan speeds with low deformation as intense energy beam of light is used as heat source. Since it requires no filler material, laser welding reduces costs[3, 4 and 5] . Titanium and titanium alloys; are widely used in many industrial fields, such as aerospace, aircraft, ship and chemical, nuclear energy and medical industries, because of many advantages such as

low specific weight, high strength, excellent corrosion resistance, attractive fracture behavior and high melting point[6-8] .

Many studies have been performed to investigate the welding performance of titanium alloys. Squillace et al [9] investigated the conduction and keyhole regime based on heat input range of Nd: YAG laser beam welding and concluded that weld morphology was highly dependent on the welding regime. Campanelli et al. [10] studied the effect of laser welding parameters on Ti6Al4V alloy and found out that the tensile strength of the joints was 80% of that of the base material, with fracture occurring in a brittle way, suggesting the need for a post-weld heat treatment to be applied on the welds. Shen et al. [11] applied laser beam welding to weld dissimilar titanium alloys, and the effect of laser beam offset on microstructural characterizations and mechanical properties of the joints were investigated .

The goal of the present work is to examine the operational reaches and stages of the welding parameters viz. pulse energy (PE), pulse on time (Ton) and welding speed (WS) on the Ultimate Tensile Strength (UTS) in Laser Nd: YAG of Titanium with Ti-6Al-7Nb Alloys and modelling of the execution measures by means of response surface methodology (RSM).

2. EXPERIMENTAL WORK

Experimental was carried out on commercial purity titanium (Ti) and Ti-6Al-7Nb with 100 × 50 mm and 1.5 mm thickness. The major chemical composition and mechanical physical properties of this alloys are listed in Table 1.

In the present investigation, all the experiments were performed on Pulse Nd-YAG laser welding as a source of laser (model Haas HL3006D), accompanied with high speed imaging (HIS), this laser is able to radiate a continuous wave mode (this mode was actually used in the experiments) with up to 3KW and predetermined were recorded using a high speed imaging system. Figure 1 show the employed laser system.

Table 1: Chemical composition of Ti and Ti-6Al-7Nb alloy used

Element	Ti	Ti-6Al-7Nb
Al	<0.005	7.0
V	0.011	<0.01
Cr	<0.005	<0.005
Cu	0.005	0.01
Fe	0.15	0.06
Mn	<0.005	0.02
Mo	<0.01	0.03
Nb	0.01	4.46
Sn	<0.02	<0.02
Ni	<0.005	0.005
Si	0.01	0.03
Zr	0.02	0.04
Pd	<0.01	<0.01
Ru	<0.01	0.01
Ti	Base	Base

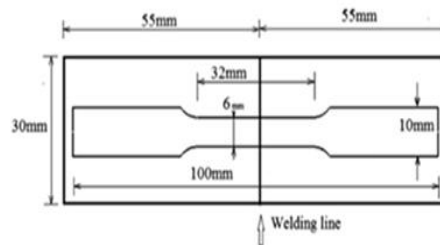


Figure 1: Show the Pulse Nd: YAG Laser Welding System, (a) Laser Welding Machine; (b) Laser Generating Device and (c) Argon Gas Tube.

A coaxial nozzle is used purging pure argon gas (purity 99.998) with the laser beam. The pulsed Nd: YAG laser has adjustable pulse shape which offers high flexibility in optimizing the weld parameters to achieve defect free joints.

After welding, the tensile strength test samples, as shown in Figure 2, were cut by wire cut operation according to the ASTM E8 standard [12].

The ultimate tensile strength (UTS) of the 30 samples were then determined using the Santam Controller universal testing machine at speed of 0.5 mm/min according to ASTM E8 standard [12].



(a)



(b)

Figure 2: Ti and Ti-6Al-7Nb Alloys Thin Sheets were Butt Welded and Wirecut as a Standard Sample for Tensile Test.

3. RESPONSE SURFACE METHODOLOGY

Response surface methodology (RSM) is a combination of mathematical, statistical method and it can be used to develop the regression model and optimization of engineering problems [13]. It is one of the Design of Experiments method used to

approximate an unknown function for which only a few values are computed. These relations are then modelled by using least square error fitting of the response surface. A Central Composite Design (CCD) is used since it gives a comparatively accurate prediction of all response variable averages related to quantities measured during experimentation [14]. CCD offers the advantage that certain level adjustments are acceptable and can be applied in the two-step chronological RSM. In these methods, there is a possibility that the experiments will stop with a few runs and decide that the prediction model is satisfactory.

In CCD, the limits of the experimental domain to be explored are defined and are made as wide as possible to obtain a clear response from the model. The WP, PE, Ton, and WS are the welding variables selected for this investigation. The different levels taken for this study are depicted in Table 2. The arrangement to conduct the experiments using a CCD with four variables, the cardinal points used are sixteen cube points, eight axial points and six center point, in total of 30 runs in three blocks [15]. The value of UTS is shown in Table 3.

The second-order model is normally used when the response function is not known or nonlinear. In the present study, a second-order model has been utilized. The experimental values are analyzed and the mathematical model is then developed that illustrate the relationship between the process variable and response. The second-order model in equation (1) explains the behaviour of the system [16].

$$Y = \beta_0 \sum_{i=1}^k \beta_i X_i + \sum_{i=1}^k \beta_{ii} X_i^2 + \sum_{i < j=2}^k \beta_{ij} X_i X_j \pm \varepsilon \quad (1)$$

Where Y is the corresponding response, X_i is the input variables, X_i^2 and $X_i X_j$ are the squares and interaction terms, respectively, of these input variables. The unknown regression coefficients are β_0 , β_i , β_{ij} and β_{ii} and the error in the model is depicted as ε .

Table 2: Input Variables used in the Experiment and their Levels

Variable	Unit	Levels		
		-1	0	1
workpieces type WP	--	AA	AB	BB
pulse energy PE	J	9	12	15
pulse duration Ton	μs	4	6	8
welding speed WS	mm/s	3	5	7

A: Ti, B: Ti-6Al-7Nb, AA: Ti + Ti,

BB: Ti-6Al-7Nb + Ti-6Al-7Nb,

AB: Ti + Ti-6Al-7Nb.

Table 3: Design Layout & Experimental Results (CCD)

No	WP	PE	Ton	WS	UTS MPa
1	-1	-1	-1	1	110
2	1	-1	-1	-1	190
3	-1	-1	1	-1	197
4	-1	1	-1	-1	212
5	1	1	-1	1	434
6	1	-1	1	1	402
7	0	0	0	0	446
8	0	0	0	0	448
9	-1	1	1	1	450
10	1	1	1	-1	776
11	0	-1	0	0	222

No	WP	PE	Ton	WS	UTS MPa
16	1	0	0	0	801
17	-1	0	0	0	426
18	0	0	1	0	496
19	0	0	0	0	444
20	0	1	0	0	466
21	-1	1	-1	1	231
22	-1	-1	1	1	214
23	0	0	0	0	445
24	-1	-1	-1	-1	101
25	-1	1	1	-1	413
26	1	-1	1	-1	370

12	0	0	0	0	447
13	0	0	0	1	407
14	0	0	0	-1	373
15	0	0	-1	0	255

27	1	1	1	1	846
28	1	1	-1	-1	398
29	1	-1	-1	1	206
30	0	0	0	0	443

The unknown coefficients are determined from the experimental data as presented in Table 4. The standard errors in the estimation of the coefficients are tabulated in the column 'SE cof.'. The F ratios are calculated for 95% level of confidence and the factors having p-value more than 0.05 are considered insignificant (shown with * in p-column). For the appropriate fitting of UTS, the non-significant terms are eliminated by the backward elimination process. The regression model is re-evaluated by determining the unknown coefficients, which are tabulated in Table 5. The model made to represent UTS depicts that WP, PE, Ton, WS, E. WP^2 , $PE^2 \times Ton^2$, WS^2 , $WP \times PE$, $WP \times Ton$ and $PE \times Ton$ are the most influencing parameters in order of significance. The final response equation for UTS is given in equation (2).

$$UTS = 451.06 + 114.94 \times WP + 123.00 \times PE + 112.61 \times T_{on} + 15.00 \times WS + 156.88 \times WP^2 - 112.62 \times PE^2 - 81.12 \times T_{on}^2 - 66.62 \times WS^2 + 37.63 \times WP \times PE + 34.13 \times WP \times T_{on} + 39.63 \times PE \times T_{on} \quad (2)$$

Table 4: Estimated Regression Coefficients for UTS (Before Backward Elimination).

Term	Coef	SE Coef	T	P
Constant	451.061	9.805	46.004	0.000
WP	114.944	7.440	15.450	0.000
PE	123.000	7.440	16.533	0.000
Ton	112.611	7.440	15.136	0.000
WS	15.000	7.440	2.016	0.062*
WP×WP	156.877	19.610	8.000	0.000
PE×PE	-112.623	19.610	-5.743	0.000
Ton×Ton	-81.123	19.610	-4.137	0.001
WS×WS	-66.623	19.610	-3.397	0.004
WP×PE	37.625	7.891	4.768	0.000
WP×Ton	34.125	7.891	4.325	0.001
WP×WS	4.500	7.891	0.570	0.577*
PE×Ton	39.625	7.891	5.022	0.000
PE×WS	5.500	7.891	0.697	0.496*
Ton×WS	4.750	7.891	0.602	0.556*
$R^2 = 98.47\%$ $R^2_{(adj.)} = 97.04\%$				

Table 5: Estimated Regression Coefficients for UTS (After backward elimination).

Term	Coef.	SE Coef.	T	P
Constant	451.06	9.294	48.533	0.000
WP	114.94	7.052	16.299	0.000
PE	123.00	7.052	17.441	0.000
Ton	112.61	7.05	15.968	0.000
WS	15.00	7.02	2.127	0.048
WP×WP	156.88	18.88	8.440	0.000
PE×PE	-112.62	18.58	-6.059	0.000
Ton×Ton	-81.12	18.5	-4.364	0.000
WS×WS	-66.62	18.17	-3.584	0.002
WP×PE	37.63	7.4	5.030	0.000
WP×Ton	34.13	7.80	4.562	0.000
PE×Ton	39.63	7.840	5.298	0.000
$R^2 = 98.35\%$ $R^2_{(adj.)} = 97.34\%$				

Since, YAG laser welding process is non-linear in nature, a linear polynomial will be not able to predict the response

accurately, and therefore the second-order model (quadratic model) is found to be adequately modelled the process. The ANOVA table for the curtailed quadratic model (Table 6) depicts the value of the coefficient of determination, R^2 as 98.35%, which signifies that how much variation in the response is explained by the model. The higher of R^2 , indicates the best fitting of the model with the data.

The model adequacy checking includes the test for significance of the regression model, model coefficients, and lack of fit, which is carried out subsequently using ANOVA on the curtailed model (Table 6). The total error of regression is the sum of errors in linear, square, and interaction terms ($961182 = 742455 + 152322 + 66405$).

Table 6: Analysis of Variance for UTS (MPa.).

Source	DF	Adj SS	Adj MS	F-Value	P-Value
Model	11	961182	87380	97.61	0.000
Linear	4	742455	185614	207.35	0.000
WP	1	237820	237820	265.66	0.000
PE	1	272322	272322	304.20	0.000
Ton	1	228263	228263	254.99	0.000
WS	1	4050	4050	4.52	0.048
Square	4	152322	38080	42.54	0.000
WP×WP	1	63763	63763	71.23	0.000
PE×PE	1	32863	32863	36.71	0.000
Ton×Ton	1	17051	17051	19.05	0.000
WS×WS	1	11500	11500	12.85	0.002
Two Way Interaction	3	66405	22135	24.73	0.000
WP×PE	1	22650	22650	25.30	0.000
WP×Ton	1	18632	18632	20.81	0.000
PE×Ton	1	25122	25122	28.06	0.000
Error	18	16113	895		
Lack-of-Fit	13	16096	1238	353.76	0.000
Pure Error	5	18	4		
Total	29	977295			

The residual error is the sum of pure and lack-of-fit errors. The fit summary recommended that the quadratic model is statistically significant for analysis of UTS. In the table, P value for the lack-of-fit is 16096, which is insignificant, so the model is certainly adequate. Moreover, the mean square error of pure error is less than that of lack-of-fit.

The final model tested for variance analysis (F-test) indicates that the adequacy of the test is established. The computed values of response parameters, model graphs are generated for the further analysis in the next section.

A complete residual analysis has been done for developing response and the graphs are shown in Fig. 3. Normal probability plot of residuals reveals that experimental data are spread approximately along a straight line, confirming a good correlation between experimental and predicted values for the response Fig.(3-a). In graph of residuals versus fitted values Fig. (3-b), only small variations can be seen. The histogram of residuals Fig.(3-c) also shows a Gaussian distribution which is desirable, and finally, in residuals against the order of experimentations in Fig. (3-d) both negative and positive residuals are apparent, indicating no special trend which is worthy from a statistical point of view. As a whole, all the yielded models do not show any inadequacy.

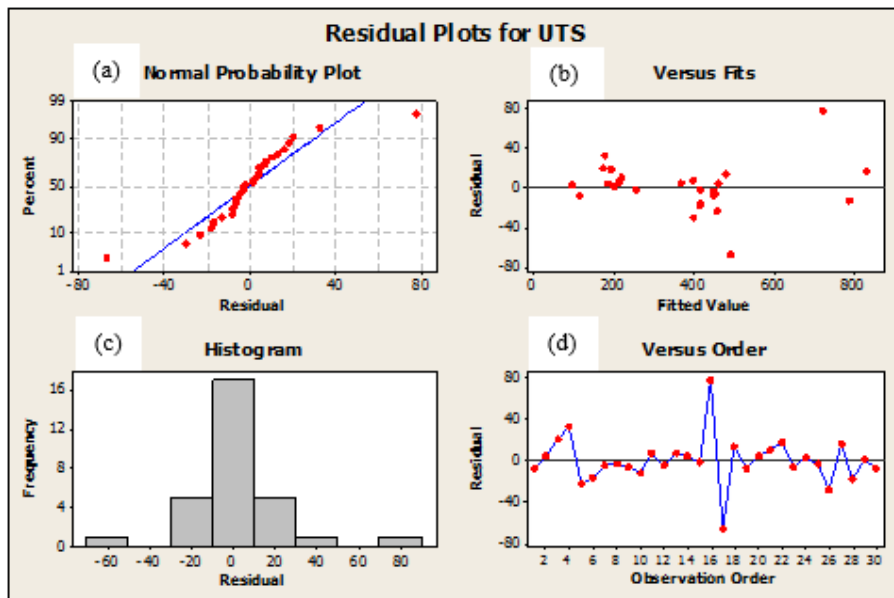


Figure 3: Residual Plot for UTS (MPa).

4. RESULTS AND DISCUSSIONS

Figure 4 depicts the main effect plots of the four controllable parameters on UTS. It is understandable that all variables have more influential impacts on UTS which is supported by results in Table 6.

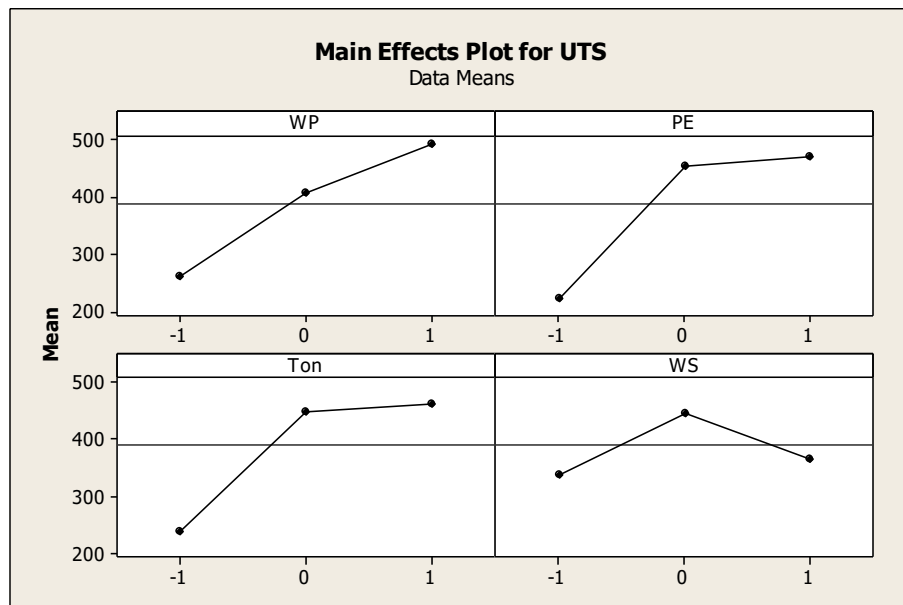


Figure 4: Main Effect Plots for UTS (MPa).

More specifically, transform the WP alone for a (Ti + Ti) to (Ti + Ti-6Al-7Nb) then (Ti-6Al-7Nb + Ti-6Al-7Nb) while keeping the other factors constant at their middle levels, can increase UTS by 88% (from 426MPa. to 801 MPa.). Because the UTS value of alloy B (Ti + Ti-6Al-7Nb) is higher than that of alloy A (Ti) [17], so the two similar BB have UTS when their laser welding is higher than AA.

In addition, UTS increases by 109 % (from 222MPa to 466MPa), with PE increases from 9J to 15J. In the other word the increase in PE causes the increase of UTS as the PE increases, specimens welded with PE 9 J were not bonded

because the PE was too low, and the molten pool did not propagate to the bottom specimen; incomplete penetration occurred. Otherwise, when the specimens were welded with high PE (15 J), the molten pool propagate to the bottom specimen; complete penetration occurred.

Similarly UTS increased by 95 % (from 255MPa to 496MPa) as the Ton increase from low to high level alone at constant middle values of other parameters. Long Ton causes the most heat transfer into the specimen. In other words, while the Ton is increased the melting isothermals penetrate further into the interior of the material, and the molten zone extends further into material and this produce a greater bonded and greater UTS.

Finally, the UTS at first increase and then decrease as the WS increases. Where it is suppose that the main reason to decrease the UTS in low level (-1) of WS is that excessive heat input is transferred in the work pieces, and consequently, lead to have vaporization instead of welding. In addition, in upper level of WS(1), with regards to high WS, there is not sufficient time to melt the material and lead to have a welding joints.

Figure 5 shows the concurrent effect of PE and WP over the UTS, (a) and (b) in 3D surface and 2D contour format. It is obviously visible that higher UTS can be obtained choosing a midmost level of PE with higher WP. This is attributed to good bonding by 12 J as well as with the Ti-6Al-7Nb + Ti-6Al-7Nb alloys, the Ti-6Al-7Nb originally has high UTS, hence the final result high UTS.

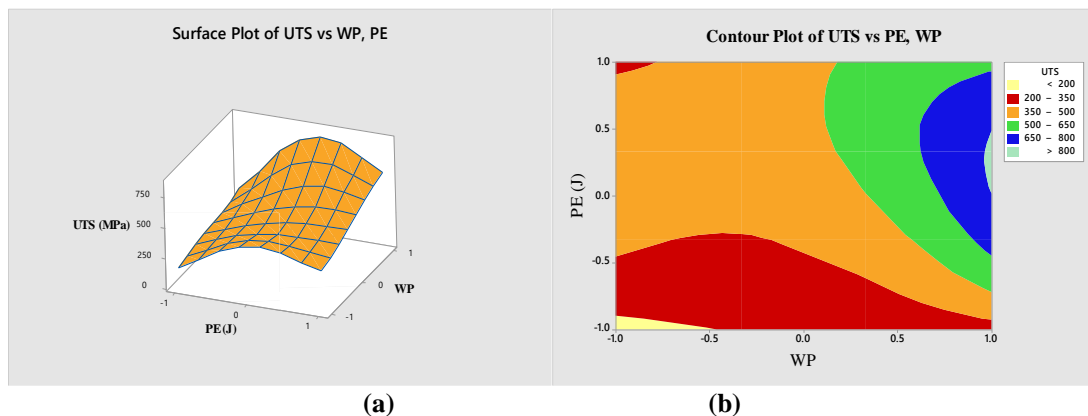


Figure 5: Response Surface Plot (a) and Contour Plot (b) UTS Versus Workpiece (WP) and Pulse Energy (PE).

The combination effect of WP and Ton at a constant level (middle value) of PE and WS has been shown in Figure 6(a) and (b) in 3D surface and 2D contour format. It can be concluded that higher UTS is achievable at the middle right region of the contour plot area where the WP at its highest level and Ton at its mid-level. This phenomenon can be attributed to high UTS of compared with other alloys, and there is enough time of the molten pool to propagate to the bottom; complete penetration occurred.

Figure 7 illustrates the combined effects of PE and Ton over the UTS. It is apparent that high UTS can be obtained allocating when the PE and Ton are at its highest levels. This can be attributed to their dominant control over the input energy.

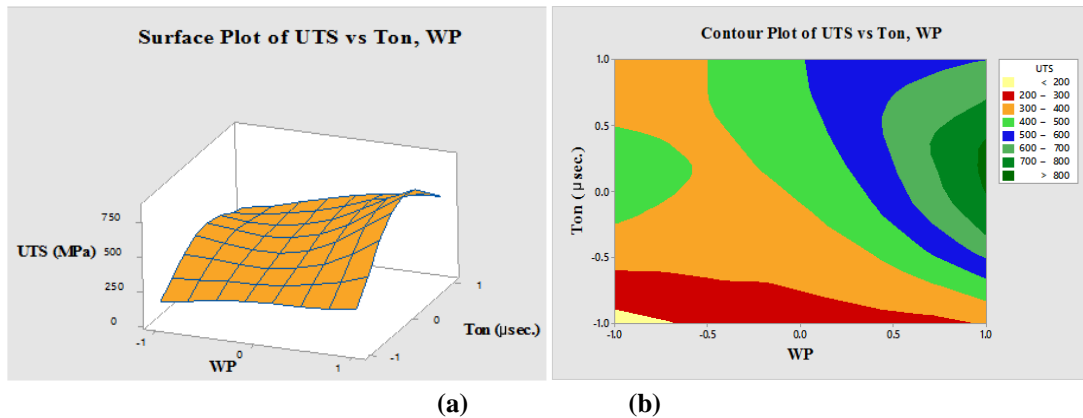


Figure 6: Response Surface Plot (a) and Contour Plot (b) UTS Versus Workpiece (WP) and Pulse Duration (Ton).

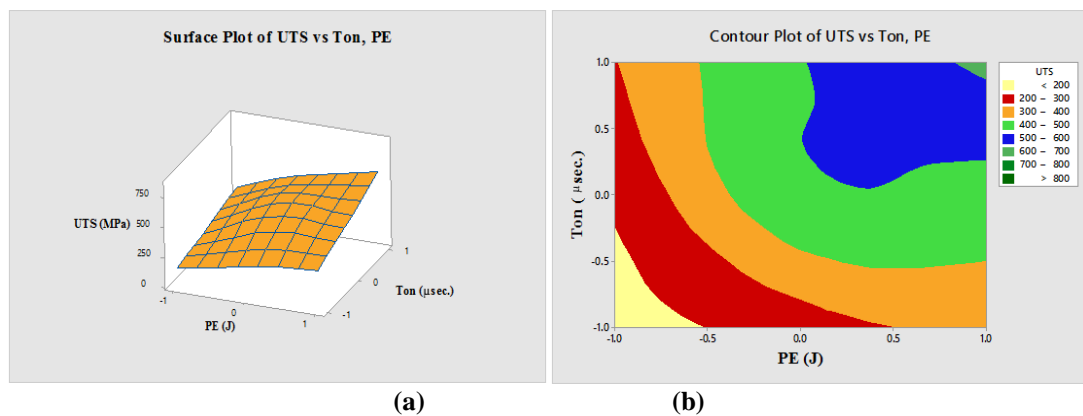


Figure 7: Response Surface Plot (a) and Contour Plot (b) UTS Versus Pulse Energy (PE) and Pulse Duration (Ton).

5. CONCLUSIONS

The following principal conclusions can be drawn:

- The input factors that significantly influenced the output responses (UTS) were the WP, PE, Ton, and WS, WP^2 , PE^2 , Ton^2 , WS^2 , $WP \times PE$, $WP \times Ton$ and $PE \times Ton$ with a confidence level of 95%.
- The result reveals that in order to obtain a high value of UTS within the work interval of this study, WP, PE, Ton, should be fixed as high as possible, whereas the WS should be fixed as middle as possible.
- The developed mathematical model for the UTS can be effectively employed for the optimal selection of the Nd: YAG laser process parameters to achieve good tensile strength of AISI 304 Titanium alloys workpieces.
- Though the Nd: YAG laser welding process parameters on Titanium alloys are highly interconnected due to its inherently complex and stochastic nature, however, the approach of RSM can beneficially help identifying process behaviour and determining appropriate Nd: YAG laser conditions meeting all performance criteria in a compromise manner.
- This research can also help researches and industries in developing a robust, reliable knowledge base and early prediction of UTS without experimenting with an Nd: YAG laser process for CP Ti with Ti-6Al-7Nb.

REFERENCES

1. Xin X., Antonio B. P., Jose A. and Juan L., 2017, "Effects of pulsed Nd: YAG laser welding parameters on penetration and microstructure characterization of a DP1000 steel Butt Joint" *Metals*, 7, 292, pp. 1-18.
2. Chintan P. M. and Ketan P., 2014, "Effect of laser welding process parameters on mechanical properties of stainless steel-316", *International Journal of Advance Engineering and Research Development*, Vol. 1, Issue 5, pp. 1-11.
3. Ceyhan K. and Engin K., 2017, "Robotic Nd: YAG Fiber Laser Welding of Ti-6Al-4V Alloy", 7, 221, pp. 1-11.
4. Nawil N., Saktioto, Fadhal M., Hussain M. S., Ali J. And Yupapin P. P. "Nd: YAG laser welding of stainless steel 304 for photonics device packaging", *Procedia Engineering*, Vol.8, pp.374-379.
5. Sandeep S. S. and Sachin M., 2017, "Research Developments in Laser Welding - A Review", *International Journal for Innovative Research in Science & Technology*, Vol. 3, Issue 11, pp. 60-64.
6. Baohua C., Zhang Y., Haitao P., Haigang L., Hao C., Dong D. and Jiguo S., 2017, "A Comparative Study on the Laser Welding of Ti6Al4V Alloy Sheets in Flat and Horizontal Positions", *Appl. Sci.* Vol. 7, Issue 4, pp. 376-388.
7. Ruifeng L., Zhuguo L. Yanyan Z. and Lei R., 2017, 2011, "Comparative study of laser beam welding and laser-MIG hybrid welding of Ti-Al-Zr-Fe titanium Alloy", *Materials Science and Engineering A* 528, pp. 1138-1142.
8. Auwal S. T., Ramesh S., Yusof F. and Manladan S. M., 2018, "A review on laser beam welding of titanium alloys", *The International Journal of Advanced Manufacturing Technology*, Vol. 97, Issue 1- 4, pp. 1071-1098.
9. Squillace A., Prisco U., Ciliberto S. and Astarita, A. 2012, "Effect of welding parameters on morphology and mechanical properties of Ti-6Al-4V laser beam welded butt joints", *J. Mater. Proc. Technol.* 212, pp. 427-436.
10. Campanelli S. L., Casalino G., Mortello M., Angelastro, A. and Ludovico, A. D. 2015, "Microstructural characteristics and mechanical properties of Ti6Al4V alloy fiber laser welds", *Procedia CIRP*, 33, pp. 429-434.
11. Shen, J., Zhang H., Hu S., Li D. and Bu, X., 2015, "Effect of laser beam offset on microstructure and mechanical properties of pulsed laser welded BTi-6431S/TA15 dissimilar titanium alloys", *Opt. Laser Technol.*, 74, pp. 158-166.
12. Standard ASTM, 2004, "Standard Test Methods for Tension Testing of Metallic Materials", *Annual Book ASTM Standards* 3, pp. 57-72.
13. Assarzadeh S. and Ghoreishi M., 2013, "Statistical modeling and optimization of the EDM parameters on WC-6%Co composite through a hybrid response surface methodology desirability function approach", *International Journal of Engineering Science and Technology*, Vol.5, No. 6, pp. 1279-1302.
14. Boopathi S. and Sivakumar K., 2014 "Study of water assisted dry wire-cut electrical discharge machining", *Indian Journal of Engineering and Materials Science*, Vol. 21, No. 1, pp. 75-82.
15. Mason R., Gunst R., Dallas, Texas and Hess J., 2003 "Statistical Design and Analysis of Experiments with Applications to Engineering and Science" Second Edition, A John Wiley & sons publication.
16. Minitab User Manual Release 16, 2013, MINITAB Inc, State College, PA, USA.
17. Mostaan H., Shamanian M., Hasani S., Safari M. and Szpunar J., 2017, "Nd: YAG laser micro-welding of ultra-thin FeCo-V magnetic alloy: optimization of weld strength", *Trans. Nonferrous Met. Soc. China* 27 (8) 1735-1746.